Simulating quantum interference in a three-level system with perpendicular transition dipole moments

Z. Ficek
Department of Physics, The University of Queensland, Brisbane, QLD 4072, Australia

S. Swain
School of Mathematics and Physics, Queen's University, Belfast BT7 1NN, United Kingdom
(Received 29 May 2003; published 2 February 2004)

We consider a three-level V-type atomic system with the ground state coupled by a laser field to only one of the excited states, and with the two excited states coupled together by a dc field. Although the dipole moments of the two dipole-allowed transitions are assumed perpendicular, we demonstrate that this system emulates to a large degree a three-level system with parallel dipole moments—the latter being a system that exhibits quantum interference and displays a number of interesting features. As examples, we show that the system can produce extremely large values for the intensity-intensity correlation function, and that its resonance fluorescence spectrum can display ultranarrow lines. The dressed states for this system are identified, and the spectral features are interpreted in terms of transitions among these dressed states. We also show that this system is capable of exhibiting considerable squeezing.

DOI: 10.1103/PhysRevA.69.023401 PACS number(s): 42.50.Hz, 32.50.+d, 42.50.Gy, 42.50.Ar

I. INTRODUCTION

Consider a three-level V-type system which interacts with the vacuum so that spontaneous decay may take place from the two excited levels to the ground state. If the system is such that the dipole moments for the two principal transitions are parallel or nearly so, then, in addition to this direct decay process, the interaction with the vacuum leads to an indirect coupling between the two excited states. Such systems have been of considerable interest since Agarwal [1] showed that spontaneous emission could be controlled by means of the quantum interference displayed by such systems. The interference results from vacuum induced coherences between the two atomic transitions: the spontaneous emission from one of the transitions modifies the spontaneous emission of the other transition. Cardimona *et al.* [2] and Hegerfeld and Plenio [3] studied the effect of quantum interference on the resonance fluorescence of such a system, and found that it can be driven into a dark state in which quantum interference prevents any fluorescence from the excited sublevels.

More recently, a number of atomic and molecular schemes have been studied and it has been demonstrated that quantum interference leads to many interesting effects which could have useful applications in spectroscopy and laser physics. These include the quenching of spontaneous emission and the presence of ultranarrow spectral lines [4–6], electromagnetically induced transparency [7], and amplification without population inversion [8]. Recent studies have also shown that quantum interference can lead to phase-dependent population inversions and phase control of spontaneous emission [9]. Keitel [10] has proposed a scheme to control the intensity of very narrow spectral lines in a V-type system driven from a single auxiliary level, which could have applications in high precision spectroscopy.

We have recently shown that quantum interference of the above type may lead to very large values of the intensity-intensity correlation function in a three-level V-type atom consisting of two excited levels coupled to a singlet ground level by electric dipole interactions [11]. The atom was driven by a single-mode laser coupled to both atomic transitions, as shown in fig.1 Previous work by Hegerfeldt and Plenio [13] for an incoherently driven atom showed that the intensity correlation may exhibit quantum beats despite the incoherent pumping. Excitation by two coherent fields was considered by Manka *et al.* [14], who showed how the resonance fluorescence and intensity-intensity correlation spectra on one transition can be influenced by the intensity of the driving field on the other transition [15].

For the coherently driven V-type atom, we found that, in the presence of quantum interference, there are extended *simultaneous* periods of darkness in the fluorescence from the two atomic transitions, even for equal decay rates of the excited levels [11]. This result is in contrast to the dark periods predicted by Cook and Kimble [16] and Pegg *et al.* [17] for a V-type atom with uncorrelated transitions and significantly different decay rates γ_1 and γ_2. In their case the atom spends most of its time in the stronger transition (large decay rate) and there is a small probability of finding the system in the other (weak) transition. In Ref. [11], we showed that for parallel dipole moments and a strong driving field, the atom emits a stream of photons exhibiting strong correlations. With near maximal quantum interference, the normalized intensity-intensity correlation function can exhibit extremely large values, whereas the corresponding value for the case of perpendicular moments is of the order of unity. Indefinitely large correlation functions for *two* two-level atoms were reported by Wiegand [18], but these large values have a different origin, due to there being positions where the field vanishes in this three-dimensional problem. Large values for the second-order intensity correlation function for nonstationary fields have been described by Jakob *et al.* [19].

However, it is difficult in practice to find suitable V-type systems with parallel dipole moments. In atoms used for

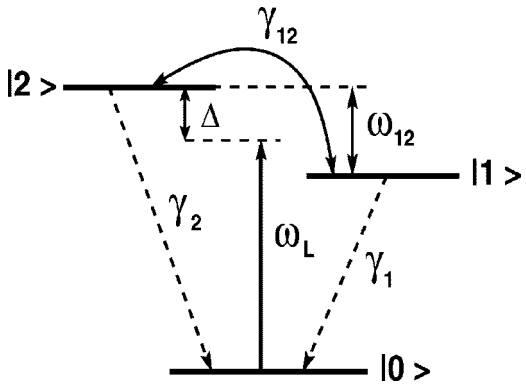

FIG. 1. Energy-level scheme of a three-level atom in the V configuration driven by a single laser field coupled to both atomic transitions (system 1).

atomic spectroscopy the dipole moments are usually perpendicular. For this reason, there have been few experimental investigations of the effects predicted. An experiment was performed [20], but it has not so far proved possible to repeat the results [21]. This experiment has also been discussed by Berman [22] and Wang *et al.* [23].

A number of different atomic schemes have been suggested for explicitly getting around this problem in the hope that they may provide a more tractable path to experimentally observing the interesting effects. Garraway and Knight [24] found that a V system coupled to a bad cavity could formally emulate the effects of quantum interference. Patnaik and Agarwal [25] showed that a four-level atom with two closely spaced intermediate states can also show the effects of quantum interference. Zhou and Swain [26] (see also Ref. [27]) demonstrated that maximal quantum interference can be achieved for a three-level atom coupled to a single-mode cavity field with pre-selected polarization in the bad cavity limit. Agarwal [28] has discussed how introducing anisotropy into the vacuum can lead to quantum interferences among the decay channels of close lying states.

In this paper, we propose an alternative scheme which permits the observation of the interesting features predicted for three-level systems showing strong quantum interference, but without the need for parallel dipole moments. In the scheme proposed here, we consider a three-level V-type atom with perpendicular dipole moments coupling the upper nearly degenerate levels with the ground level. We assume that one of the atomic dipole transitions is driven by a strong laser field and a dc field is applied to the atom to couple the upper levels. Dalton and Gagen [29] and Hakuta *et al.* [30] considered a similar scheme in which the dc field coupled a driven transition to a metastable level. In our scheme, we relax the condition that the third level *must* be metastable, allowing a nonzero spontaneous decay to the ground state. This broadens the range of interesting quantum interference effects it is possible to observe in three-level atoms.

II. THE THREE-LEVEL SYSTEM

In Ref. [11] we have considered photon correlations in a three-level system in the V configuration as shown in Fig. 1. The atom consists of two nondegenerate excited levels $|1\rangle$ and $|2\rangle$ separated from the ground level $|0\rangle$ by transition frequencies ω_1 and ω_2, and connected by the electric dipole moments $\vec{\mu}_1$ and $\vec{\mu}_2$, respectively. We assume that the excited sublevels can decay to the level $|0\rangle$ by spontaneous emission, whereas direct spontaneous transitions between the excited sublevels are dipole forbidden.

In the frame rotating with the laser frequency ω_L the master equation is of the form

$$\dot{\rho} = -i[\rho, H] + \mathcal{L}\rho, \tag{1}$$

where the Hamiltonian is

$$H = (\Delta - \omega_{12})A_{11} + \Delta A_{22} + [(\Omega_1 A_{10} + \Omega_2 A_{20}) + \text{H.c.}], \tag{2}$$

and the damping term is

$$\mathcal{L}\rho = \frac{1}{2}\gamma_1(2A_{01}\rho A_{10} - A_{11}\rho - \rho A_{11}) + \frac{1}{2}\gamma_2(2A_{02}\rho A_{20} - A_{22}\rho - \rho A_{22}) + \frac{1}{2}\gamma_{12}(2A_{01}\rho A_{20} - A_{21}\rho - \rho A_{21}) + \frac{1}{2}\gamma_{12}(2A_{02}\rho A_{10} - A_{12}\rho - \rho A_{12}). \tag{3}$$

In these equations, $A_{ij} \equiv |i\rangle\langle j|$ is the transition operator, $\Delta = \omega_2 - \omega_L$ is the detuning between the frequency ω_2 of the $|0\rangle \rightarrow |2\rangle$ transition and the driving laser frequency, $2\Omega_k (k = 1,2)$ is the Rabi frequency of the kth transition ($k = 1,2$), and $\omega_{12} = \omega_1 - \omega_2$ is the level splitting between the excited sublevels. Here γ_i is the spontaneous decay constant of the excited sublevel $|i\rangle$ ($i = 1,2$) to the ground level $|0\rangle$, while

$$\gamma_{ij} = \frac{2\sqrt{\omega_i^3 \omega_j^3}}{3\hbar c^3}\vec{\mu}_i \cdot \vec{\mu}_j = \beta\sqrt{\gamma_i \gamma_j} \quad (i \neq j = 1,2) \tag{4}$$

arises from the cross damping (quantum interference) between the transitions $|1\rangle \rightarrow |0\rangle$ and $|2\rangle \rightarrow |0\rangle$. The cross damping term (4) is sensitive to the mutual orientation of the atomic transition dipole moments, which is represented here by the parameter β, the cosine of the angle between the two dipole moment vectors. If the dipole moments are parallel, $\beta = 1$, then the cross damping term is maximal with $\gamma_{12} = \sqrt{\gamma_1 \gamma_2}$, while $\gamma_{12} = 0$ if, as is usually the case, the dipole moments are perpendicular ($\beta = 0$), and the quantum interference term vanishes.

It is evident from the form of the Liouvillean $\mathcal{L}$ that the spontaneous decay in this system is *off diagonal*—that is, the equation of motion for the density matrix element ρ_{ij} will contain damping terms that are proportional to ρ_{kj} and/or ρ_{ik}, in addition to the diagonal damping terms proportional to ρ_{ij}. We showed in Ref. [11] that if we transform to a new basis characterized by the following symmetric and antisymmetric superposition states of the excited levels:

$$|s\rangle = \frac{1}{\sqrt{\gamma_1+\gamma_2}}(\sqrt{\gamma_1}|1\rangle + \sqrt{\gamma_2}|2\rangle),$$

$$|a\rangle = \frac{1}{\sqrt{\gamma_1+\gamma_2}}(\sqrt{\gamma_2}|1\rangle - \sqrt{\gamma_1}|2\rangle), \tag{5}$$

the off-diagonal damping terms become proportional to $\gamma_1 - \gamma_2$. A more detailed discussion is given in Ref. [12].

For simplicity, we henceforth consider the case where $\gamma_1 = \gamma_2 = \gamma$, when the damping becomes purely diagonal, and we also assume $\Omega_2 = \Omega_1 = \Omega$. The symmetric and antisymmetric superposition states of the excited levels then become simply

$$|s\rangle = \frac{1}{\sqrt{2}}(|1\rangle + |2\rangle),$$

$$|a\rangle = \frac{1}{\sqrt{2}}(|1\rangle - |2\rangle), \tag{6}$$

and the decay term in Eq. (1) is diagonalized. The master equation (1) and the Hamiltonian (2) take the form:

$$\dot{\rho} = -i[\rho, H] + \frac{1}{2}\gamma(1+\beta)(2A_{0s}\rho A_{s0} - A_{ss}\rho - \rho A_{ss})$$

$$+ \frac{1}{2}\gamma(1-\beta)(2A_{0a}\rho A_{a0} - A_{aa}\rho - \rho A_{aa}), \tag{7}$$

with

$$H = \Delta_1(A_{ss} + A_{aa}) - \frac{1}{2}\omega_{12}(A_{sa} + A_{as}) + \sqrt{2}\Omega(A_{s0} + A_{0s}), \tag{8}$$

and

$$\Delta_1 = \Delta - \frac{1}{2}\omega_{12}. \tag{9}$$

It is apparent that the laser field couples only to the symmetric state and both states decay independently to the ground state with different decay rates. In fact, if the dipole moments are almost parallel, so that $\beta \simeq 1$, it is clear that the antisymmetric level is metastable. If the original levels $|1\rangle$ and $|2\rangle$ are degenerate, the coupling between the symmetric and antisymmetric states vanishes.

If we ignore the $\Delta_1 A_{aa}$ term in Eq. (8), we observe that the system described by Eqs. (7) and (8) is equivalent to that of a three-level system in which the ground state $|0\rangle$ is connected to the excited state $|s\rangle$ by a laser field detuned from resonance with the state $|s\rangle$ by the amount Δ_1, while $|s\rangle$ is also connected with the other excited state, $|a\rangle$, for example, by a dc field.

In the remainder of this paper, we consider a generalization of this system in which we allow the two excited states to be nondegenerate, and their decay rates to the ground state to be arbitrary. We also redefine the coupling constants to be equal to twice the corresponding Rabi frequencies, and we denote the ground state henceforth as $|g\rangle$, rather than $|0\rangle$,

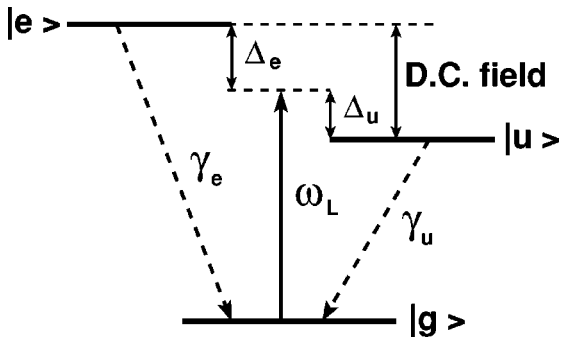

FIG. 2. Energy-level scheme of the three-level atom (system 2). The single laser couples only one of the atomic dipole transitions, while a dc field couples the two excited states.

and the upper states as $|e\rangle$ and $|u\rangle$. Explicitly the system we consider is described, in the rotating frame, by the Hamiltonian

$$H = \Delta_e A_{ee} + \Delta_u A_{uu} - D(A_{eu} + A_{ue}) + \Omega(A_{eg} + A_{ge}), \tag{10}$$

and Liouvillean

$$\mathcal{L}\rho = \frac{1}{2}\gamma_e(2A_{ge}\rho A_{eg} - A_{ee}\rho - \rho A_{ee})$$

$$+ \frac{1}{2}\gamma_u(2A_{gu}\rho A_{ug} - A_{uu}\rho - \rho A_{uu}), \tag{11}$$

where D is the Rabi frequency of the dc field directly coupling the upper states.

This system, shown in Fig. 2, is the one studied in detail in this paper. Comparing Eqs. (7) and (11), we define

$$\beta = \cos^{-1}\theta = (\gamma_e - \gamma_u)/(\gamma_e + \gamma_u) \tag{12}$$

as a measure of quantum interference. We thus expect that the level $|u\rangle$ has to be metastable ($\gamma_u \ll \gamma_e$) if we are to see maximal effects of quantum interference.

However, we wish to investigate how far the effects of quantum interference are duplicated by the latter system when the detunings are unequal, when there is no unitary equivalence with system 1, and when we relax the condition $\gamma_u \ll \gamma_e$. In the following sections we shall show that the system described by Eqs. (10) and (11), to be referred to henceforth as system 2, behaves in a rather similar way to the original system (1) [or equivalently, system (7)], to be referred to as system 1. However, system 1 requires dipole moments that are almost parallel, while perpendicular moments are assumed for system 2.

III. INTENSITY-INTENSITY CORRELATION FUNCTION

We demonstrated in Ref. [11] that system 1 can exhibit extraordinarily large values of the normalized intensity-intensity correlation function. Here, we show that system 2 exhibits a similar type of behavior. The normalized intensity-intensity correlation function is defined by

$$g^{(2)}(t,t+\tau)=\frac{G^{(2)}(t,\tau)}{G^{(1)}(t)G^{(1)}(t+\tau)}. \tag{13}$$

The first- and second-order correlation functions, appearing in Eq. (13), can be expressed in terms of the positive and negative frequency parts of the electric-field operator as

$$G^{(1)}(t)=k\langle\vec{E}_+(t)\vec{E}_-(t)\rangle, \tag{14}$$

$$G^{(2)}(t,\tau)=k^2\langle\vec{E}_+(t)\vec{E}_+(t+\tau)\vec{E}_-(t+\tau)\vec{E}_-(t)\rangle. \tag{15}$$

We later choose a convenient value for the arbitrary positive constant k. $G^{(2)}(t,\tau)$ is a relative measure of the joint probability that a photon is detected at time $t+\tau$ if one was detected at time t.

The electric field may be expressed as a vacuum term plus a term radiated by the atom. Since the field is initially in the vacuum state, the vacuum part does not contribute to the expectation values of the normally ordered field operators and then for the purpose of evaluating the correlation functions, we may take

$$\vec{E}_-(t)\propto\vec{\mu}_{ug}A_{ug}(t)+\vec{\mu}_{eg}A_{eg}(t), \tag{16}$$

where $A_{ig}=|i\rangle\langle g|, i=e,u$ is the transition operator between the excited and ground levels and $\vec{\mu}_{ig}$ is the corresponding dipole moment. Since in system 2 we assume that the dipole moments of the atomic spontaneous transitions are perpendicular, we obtain the following expressions for the correlation functions:

$$G^{(1)}(t)=\sum_{i=e,u}\gamma_i\langle A_{ii}(t)\rangle, \tag{17}$$

and

$$G^{(2)}(t,\tau)=\sum_{i,j=e,u}\gamma_i\gamma_j\langle A_{ig}(t)A_{jj}(t+\tau)A_{gi}(t)\rangle, \tag{18}$$

where γ_i is the spontaneous decay constant of the excited sublevel $|i\rangle$ $(i=e,u)$ to the ground level $|g\rangle$. [We have chosen the value of the constant k in order that the spontaneous decay rates γ_i are the coefficients that appear in Eqs. (17) and (18).]

Noting that $\langle A_{ig}(t)A_{jj}(t+\tau)A_{gi}(t)\rangle$ may be written

$$\begin{aligned}\langle A_{ig}(t)A_{jj}(t+\tau)A_{gi}(t)\rangle&=\langle i|\rho(t)|i\rangle|\langle j|U(\tau)|g\rangle|^2\\&=P_i(t)P(g,0\rightarrow j,\tau),\end{aligned} \tag{19}$$

where $P(g,0\rightarrow j,\tau)$ is the probability that if the system is in the ground state $|g\rangle$ at time $t=0$ it will be in the excited state $|j\rangle$ at time $t=\tau$, $U(t)$ is the time-development operator, and $P_i(t)$ is the probability that the system will be in state $|i\rangle$ at time t, we may express the normalized intensity-intensity correlation function $g^{(2)}(t,t+\tau)$ as

$$g^{(2)}(t,\tau)=\frac{\gamma_uP(g,0\rightarrow u,\tau)+\gamma_eP(g,0\rightarrow e,\tau)}{\gamma_uP_u(t+\tau)+\gamma_eP_e(t+\tau)}. \tag{20}$$

Henceforth, we assume that we are dealing with stationary fields in the steady-state situation, $t\rightarrow\infty$, when $P_i(t)$ becomes independent of time. We may then write

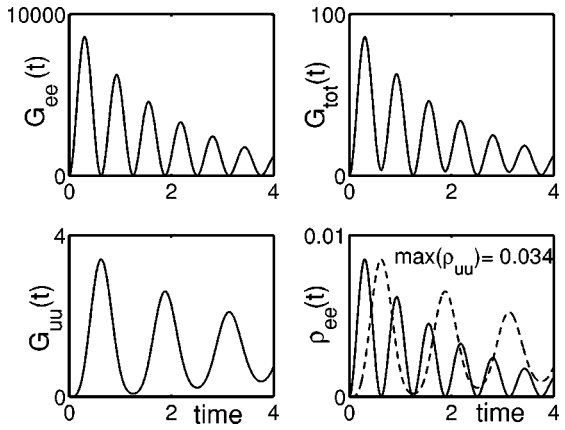

FIG. 3. Second-order intensity-intensity correlation functions and the density matrix elements for $D=5$, $\Omega=0.5$, $\Delta_e=\Delta_u=0$, and $\gamma_u=0.01$. The fourth frame shows ρ_{ee} as a solid line. The dotted line represents $[\rho_{uu}(t)/\max(\rho_{uu})]\max(\rho_{ee})$. To enable absolute values of ρ_{uu} to be estimated, its maximum value is indicated in the fourth frame. In this and all subsequent figures, $\gamma_e=1$.

$$g^{(2)}_{tot}(\tau)=\frac{\gamma_uP(g,0\rightarrow u,\tau)+\gamma_eP(g,0\rightarrow e,\tau)}{\gamma_uP_u+\gamma_eP_e}, \tag{21}$$

where $P_i=\lim_{t\rightarrow\infty}P_i(t)$, and we have added the subscript *tot* to emphasize that in writing down Eq. (21) we have assumed that our photodetector responds to the total field incident upon it, as evinced by our use of the expression (16).

It is, however, possible in principle to arrange the photodetector so that it responds only to photons emitted on the $|e\rangle\rightarrow|g\rangle$ transition, or only to photons emitted on the $|u\rangle\rightarrow|g\rangle$ transition, when the corresponding correlation functions measured are

$$g^{(2)}_{jj}(\tau)=\frac{P(g,0\rightarrow j,\tau)}{P_j}, \quad j=e,u. \tag{22}$$

The value of $P(g,0\rightarrow j,\tau)$ is calculated by solving the master equation for ρ_{jj} subject to the initial conditions $\rho(0)=|g\rangle\langle g|$. We illustrate the features of these correlation functions in the following figures. In all cases, we measure quantities as ratios of γ_e (i.e., we take $\gamma_e=1$), and throughout this section we take $D=5$, $\Omega=0.5$.

In Fig. 3 we take $\gamma_u=0.01$, $\Delta_e=\Delta_u=0$. In this case, system 1 is unitarily equivalent to system 2, with the dipole moments almost parallel [cf. Eq. (12)]. The first two frames show that $g^{(2)}_{tot}$ and $g^{(2)}_{ee}$ exhibit very strong photon correlations, as expected, while $g^{(2)}_{uu}$ as shown in the third frame exhibits much weaker correlations. Although the steady-state diagonal density-matrix elements ρ_{ee} and ρ_{uu} are proportional to $g^{(2)}_{ee}$ and $g^{(2)}_{uu}$, respectively, they are shown separately in the final frame. ρ_{ee} is represented by the solid line. For clarity, we have normalized ρ_{uu} to the same maximum value as ρ_{ee}. That is, the dotted line represents $\rho_{uu}(t)/\max(\rho_{uu})\times\max(\rho_{ee})$. To enable the absolute values of $\rho_{uu}(t)$ and ρ_{ee} to be compared, the maximum value of $\rho_{uu}(t)$ is shown in the frame.

For this small value of γ_u, we note that

(i) $g^{(2)}_{tot}$ is qualitatively similar to $g^{(2)}_{ee}$,
(ii) the oscillations in $g^{(2)}_{ee}$ are twice as rapid as those in $g^{(2)}_{uu}$,
(iii) both ρ_{ee} and ρ_{uu} exhibit simply harmonic oscillations.

Property (i) holds because the first term in Eq. (21) dominates the second for these parameter values [$\gamma_u/\gamma_e = 0.01$, $\max(\rho_{ee})/\max(\rho_{uu}) \simeq 0.25$]. The very large values of $g^{(2)}_{ee}$ are due to the normalization employed in Eq. (22). For short times, the maximum values of $\rho_{ee}(t)$ are of order 0.01, whereas the steady-state value is $\rho_{ee}(\infty) \simeq 10^{-6}$.

The properties of this system may be partially understood by considering the special case $\Delta_u = \gamma_u = 0$. That is, we assume the laser is resonant with level $|u\rangle$, which is completely stable. It is then very easy to show that the steady-state solution is

$$\rho_{ee} = \rho_{eu} = \rho_{eg} = 0,$$
$$\rho_{uu} = \frac{\Omega^2}{D^2+\Omega^2}, \quad \rho_{ug} = \frac{\Omega D}{D^2+\Omega^2}. \tag{23}$$

Thus the system eventually evolves into the pure state

$$|\Psi\rangle = \frac{D|g\rangle + \Omega|u\rangle}{\sqrt{D^2+\Omega^2}}, \tag{24}$$

independently of the values of Δ_e and γ_e and of the initial state of the system. Although the laser is driving the transition $|g\rangle \rightarrow |e\rangle$, there is no population in the state $|e\rangle$ in the steady state in spite of the ground state $|g\rangle$ being populated, and the system is ''dark''— i.e., no radiation at all is emitted. We have a coherent population trapping situation.

However, if we consider the evolution of the system from the initial density matrix

$$\rho(\tau = 0) = |g\rangle\langle g| \tag{25}$$

[so that $\rho_{jj}(\tau) = P(g,0 \rightarrow j,\tau)$, as appears in Eq. (20)] there will for short times be population in the state $|e\rangle$, and fluorescence will occur. For $\gamma_u = 0$, one cannot define the steady-state intensity-intensity correlation function, as all the relevant quantities are zero. It would, however, be meaningful to define *transient* intensity-intensity correlation functions, but we do not consider these here [19].

If we now suppose γ_u to be small but nonzero, then there will be fluorescence even in the steady state, but the mean number of photons emitted in unit time will be very small. If we concentrate on the photons emitted on the $|e\rangle \rightarrow |g\rangle$ transition for definiteness, then the steady-state value of ρ_{ee} will be very small, while $P(g,0 \rightarrow e,\tau)$ will be much larger for shorter times. Thus the short-time values of $g^{(2)}(\tau)$ will be very large. According to the expressions (23), we expect these values to become larger if the ratio Ω/ω increases, and this we find to be so in our numerical investigations.

If we increase the value of γ_u to $\gamma_u = 0.1$, we find that properties (i) and (iii) still hold, but that $g^{(2)}_{tot}$ is no longer qualitatively similar to $g^{(2)}_{ee}$. It clearly shows a doubly peaked structure. This is because the relative weights of the two terms in the numerator of Eq. (21) become comparable [$\gamma_u/\gamma_e = 0.1$, $\max(\rho_{ee})/\max(\rho_{uu}) \simeq 0.26$]. The form of $g^{(2)}_{tot}$ shows that it is composed of the sum of two oscillations of different frequencies.

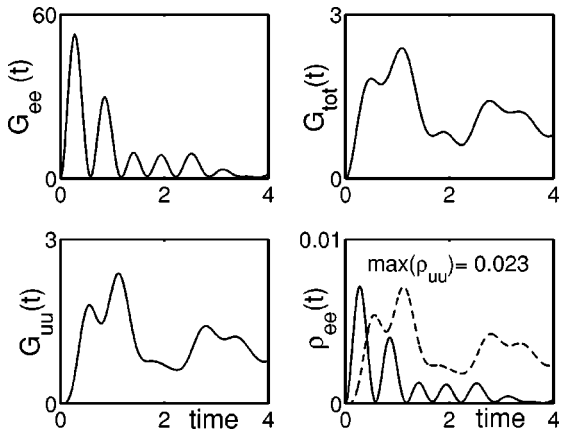

FIG. 4. Second-order intensity-intensity correlation functions as in Fig. 3, except that $\gamma_u = 1$, $D = 5$, $\Omega = 0.5$, $\gamma_u = 1$, $\Delta_e = 5$, and $\Delta_u = 0$.

Next, we investigate the effect of finite detunings. For example, we keep the same parameter values as in Fig. 3, except for assuming that $\gamma_u = 0.1$, and introduce the finite detunings $\Delta_u = 5$, $\Delta_e = 0$. The system is then no longer unitarily equivalent to system 1. We find numerically that there is no appearance of single-harmonic behavior in any of the three correlation functions. The maximum amplitudes of $g^{(2)}_{tot}$ and $g^{(2)}_{ee}$ are much reduced, to an unremarkable value of about 4. The systems $\{|e\rangle, |g\rangle\}$ and $\{|u\rangle, |0\rangle\}$ cannot be considered to behave as two independent, effective two-level systems.

If, however, we take $\Delta_u = 0$ and $\Delta_e = 5$, we find that the very large maximum amplitude of $g^{(2)}_{ee}$ is restored, although not quite to such large values as when both detunings were zero.

Finally, we investigate increasing the value of γ_u. If we keep the detunings $\Delta_u = 0$ and $\Delta_e = 5$, but increase the value of γ_u to $\gamma_u = 1$, we still obtain large values for $g^{(2)}_{ee}$, although the oscillations are no longer singly harmonic. This is rather surprising at first, as $|u\rangle$ can no longer be considered a metastable level. However, the steady-state population of $|e\rangle$ is still much smaller than the steady-state population of $|u\rangle$, but this is now due to the detuning of the $|e\rangle \rightarrow |g\rangle$ transition from resonance. Thus we can dispense with the requirements that $|u\rangle$ be metastable, and $|e\rangle$ and $|u\rangle$ be degenerate, and still obtain large values for $g^{(2)}_{ee}$. These features are illustrated in Fig. 4.

IV. RESONANCE FLUORESCENCE SPECTRA AND SQUEEZING

A. Numerical calculations

Another interesting feature of system 1 is that it has been shown to exhibit very sharp peaks in the incoherent fluorescence spectrum under certain conditions. We show that this feature is also shared by system 2. We consider the case

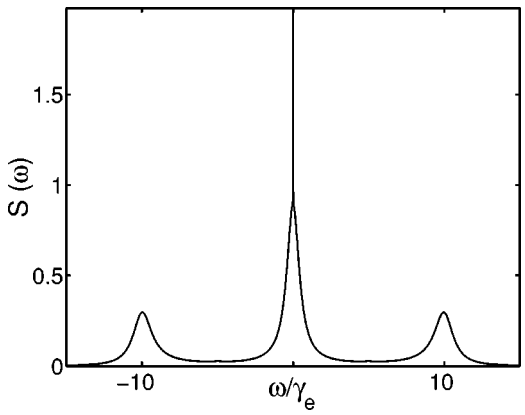

FIG. 5. The resonance fluorescence spectrum $S(\omega)$ for $\Omega=5$, $D=0.25$, $\Delta_e=\Delta_u=0$, and $\gamma_u=0.001$.

$\Delta_u=\Delta_e=0$, taking $\gamma_u=0.001$, in Fig. 5 which shows the existence of an ultranarrow line at the center of the resonance fluorescence spectrum. The sharpness of the line is decreased by increasing the value of γ_u. (The spectrum is actually five peaked, but the inner side peaks are so small as to be barely noticeable in the figure.) We emphasize that the sharp line shown in Fig. 5 is due to incoherent scattering, as the coherent contribution has been excluded from our figures.

The ratio of the relative weight of the inner side peaks to the outer side peaks increases with the value of D/Ω, as we show in Fig. 6. In this case, the five-peaked nature of the spectrum is obvious, and the fluorescence spectrum does not exhibit the sharp line at the central frequency.

We point out that the system can show strong squeezing under appropriate conditions, as we demonstrate in Fig. 7, where we plot the squeezing spectrum for the in-phase and out-of-phase quadratures. It can also be shown that the ultranarrow lines persist in the presence of detunings. The ultrasharp peak amplitude can be enhanced by allowing Δ_e to become negative. In this example, the resonance fluorescence spectrum reverts to a three-peaked one. It is worth noting that the squeezing is approximately independent of

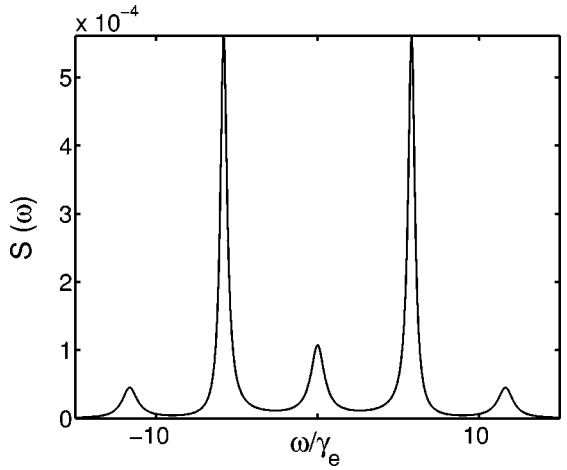

FIG. 6. The in-phase $S_1(\omega)$ and out-of-phase $S_2(\omega)$ squeezing spectra, and the resonance fluorescence spectrum $S(\omega)$ for $D=5$, $\Omega=5$, $\Delta_e=\Delta_u=0$, and $\gamma_u=1$.

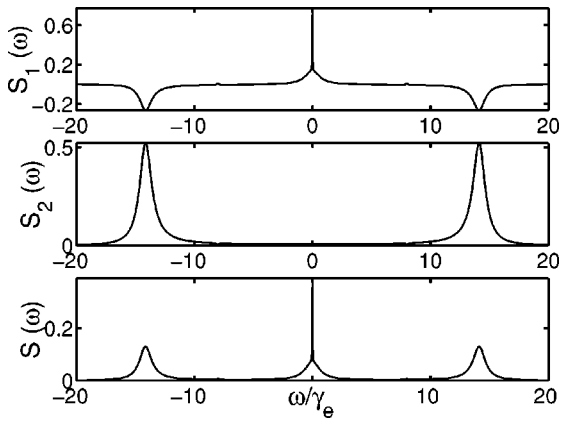

FIG. 7. The in-phase and out-of-phase squeezing spectra, and the resonance fluorescence spectrum for $D=1$, $\Omega=5$, $\Delta_e=-10$, $\Delta_u=10$, and $\gamma_u=0.01$.

the value of γ_u. Thus if we increase the value of γ_u to $\gamma_u=1$, leaving all the other parameters as in Fig. 7, then the degree of squeezing is unchanged (but the ultra sharp peak disappears).

B. Dressed-atom explanation of the spectral features

In Sec. IV A we presented the incoherent fluorescence spectrum for system 2 with $\gamma_u \ll \gamma_e$. Here, we give an explanation of the spectral features in terms of the dressed states of the system, and the transitions among them. We perform the calculations using the dressed-atom technique developed by Cohen-Tannoudji and Reynaud [34], and extended by Dalton and Gagen [29] to a three-level system with permanent dipole moments created in the upper states by dc coupling. In this approach, the laser field is treated quantum mechanically and the eigenstates of the Hamiltonian of the combined atom and driving-field system are found and used as the basis for further calculations. The method is essentially based on the original master equation (7) but with the unperturbed Hamiltonian (10) modified to include the free-field Hamiltonian for the laser field and the atom-field interaction replaced by a fully quantum coupling. Since the dc field does not affect the optical photon modes, we treat the atom-dc field interaction semi-classically (quantum atomic operators and *c*-number dc field). While it is possible to treat the problem with full generality using the dressed-atom picture, in the interests of having simple, transparent expressions to deal with, we restrict ourselves [31–33] to the situation in which the laser field and the dc field are in exact resonance with their respective transitions. (The resonance fluorescence spectra obtained in the exact resonance case can exhibit no more than five peaks, whereas in the general case, there may be up to seven peaks.)

In the case of exact resonance, the Hamiltonian of the atom interacting with the quantized laser field and the dc field may be written as

$$H=H_{al}+H_{dc}, \tag{26}$$

where

$$H_{al}=\hbar\omega_L(|e\rangle\langle e|+|u\rangle\langle u|+\hat{a}_L^\dagger\hat{a}_L)+\hbar v(A_{eg}\hat{a}_L+\hat{a}_L^\dagger A_{ge}) \tag{27}$$

is the Hamiltonian of the atom and the laser field component, and

$$H_{dc}=-\hbar D(A_{eu}+A_{ue}) \tag{28}$$

is the interaction between the laser driven atom and the dc field.

The Hamiltonian (27) has eigenstates $|u,N-1\rangle,|1,N\rangle,|2,N\rangle$ satisfying the eigenvalue equations

$$\begin{aligned} H_{al}|u,N\rangle&=\hbar N\omega_L|u,N\rangle,\\ H_{al}|1,N\rangle&=\hbar(N\omega_L-\Omega)|1,N\rangle,\\ H_{al}|2,N\rangle&=\hbar(N\omega_L+\Omega)|2,N\rangle, \end{aligned} \tag{29}$$

where

$$\begin{aligned} |u,N\rangle&=|u\rangle|N-1\rangle,\\ |1,N\rangle&=\frac{1}{\sqrt{2}}(|g\rangle|N\rangle+|e\rangle|N-1\rangle),\\ |2,N\rangle&=\frac{1}{\sqrt{2}}(|g\rangle|N\rangle-|e\rangle|N-1\rangle) \end{aligned} \tag{30}$$

are the atom-laser field dressed states, N is the number of photons in the laser mode, and $2\Omega=2v\sqrt{N}$ is the Rabi frequency of the laser field. The states (30) form a ladder of triplets with adjacent triplets separated by ω_L, and intratriplet splitting 2Ω.

When we include the interaction H_{dc} between the atom-laser field dressed states and the dc field, the triplets recombine into new triplets with eigenstates

$$\begin{aligned} |0,N\rangle&=a|g,N\rangle+b|u,N-1\rangle,\\ |+,N\rangle&=\frac{1}{\sqrt{2}}(b|g,N\rangle+|e,N-1\rangle-a|u,N-1\rangle),\\ |-,N\rangle&=\frac{1}{\sqrt{2}}(b|g,N\rangle-|e,N-1\rangle-a|u,N-1\rangle), \end{aligned} \tag{31}$$

corresponding to energies

$$\begin{aligned} E_{N,0}&=\hbar\omega_L,\\ E_{N,+}&=\hbar(\omega_L+\Omega'),\\ E_{N,-}&=\hbar(\omega_L-\Omega'), \end{aligned} \tag{32}$$

where

$$a=\frac{D}{\Omega'},\quad b=\frac{\Omega}{\Omega'}, \tag{33}$$

and

$$2\Omega'=2\sqrt{\Omega^2+D^2} \tag{34}$$

is the effective Rabi frequency of the driving fields.

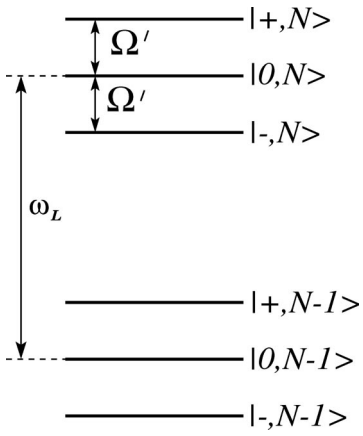

FIG. 8. Dressed states of two neighboring manifolds $|N\rangle$ and $|N-1\rangle$.

The dressed states of the system form a ladder of triplets, as shown in Fig. 8, with adjacent triplets separated by ω_L, while the intratriplet separation is Ω'.

Having available the dressed states of the system, we can find the frequencies and amplitudes of the spontaneous transitions between the dressed states. Considering the energy diagram, Fig. 8, and Eq. (32), it is apparent that the possibility of fluorescence exists at the five distinct frequencies

$$\omega_{ij}=\hbar^{-1}(E_{N,i}-E_{N-1,j}), \tag{35}$$

given explicitly as

$$\begin{aligned} \omega_{00}&=\omega_{++}=\omega_{--}=\omega_L,\\ \omega_{0-}&=\omega_{+0}=\omega_L+\Omega',\\ \omega_{0+}&=\omega_{-0}=\omega_L-\Omega',\\ \omega_{+-}&=\omega_L+2\Omega',\\ \omega_{-+}&=\omega_L-2\Omega'. \end{aligned} \tag{36}$$

These frequencies correspond exactly to the frequencies of the spectral lines presented in Figs. 5 and 6. For example, in Fig. 6, the inner (outer) sidebands appear at frequencies $\pm 5.8\gamma_e(\pm 11.6\gamma_e)$. With the parameters of Fig. 6, the dressed atom transition frequencies (36) and Eq. (34) predict exactly the same values for the frequencies of the inner and outer sidebands.

In order to calculate the intensities of the spectral features, we have to calculate populations of the dressed states and transition rates between the dressed states of two neighboring manifolds. The transition rates are proportional to the absolute square of the dipole transition moment connecting them [34],

$$\gamma_{ij}=\gamma_e|\langle i,N|A_{eg}|j,N-1\rangle|^2+\gamma_u|\langle i,N|A_{ug}|j,N-1\rangle|^2. \tag{37}$$

Using Eqs. (31) and (37), we find that the transition rates between $|i,N\rangle$ and $|j,N-1\rangle$ are

$$\begin{aligned} \gamma_{00}&=a^2b^2\gamma_u,\\ \gamma_{0+}&=\gamma_{0-}=\frac{1}{2}b^4\gamma_u, \end{aligned} \tag{38}$$

$$\gamma_{++}=\gamma_{--}=\frac{1}{2}b^2\Gamma,$$

$$\gamma_{+-}=\gamma_{-+}=\frac{1}{2}b^2\Gamma,$$

$$\gamma_{+0}=\gamma_{-0}=a^2\Gamma,$$

where $\Gamma=(\gamma_e+a^2\gamma_u)/2$.

It is seen that in the limit of $\gamma_u=0$, the transition rates from the state $|0,N\rangle$ are all zero. Since the transition rates into the state $|0,N\rangle$ from the dressed states of the manifold above are nonzero, the population will be trapped in this state. This is the population trapping effect considered by Dalton and Gagen [29]. In the numerical calculations presented in Sec. IV A, we have computed quantum interference effects that do not depend upon the assumption $\gamma_u=0$.

To analyze the intensities of the spectral lines we need the steady-state populations of the dressed states. We use the master equation (7) to find the time evolution of the populations of the dressed states. We project the master equation onto $|i,N\rangle$ on the right and $\langle i,N|$ on the left, make the secular approximation in which we ignore couplings between populations and coherences, and introduce the ''reduced populations'' [34]

$$P_i=\sum_N \langle i,N|\rho|i,N\rangle. \tag{39}$$

The population equations then reduce to three coupled equations

$$\begin{aligned}
\dot{P}_0&=-b^4\gamma_u P_0+a^2\Gamma(P_++P_-),\\
\dot{P}_+&=-\left(1-\frac{b^2}{2}\right)\Gamma P_++\frac{b^2\Gamma}{2}P_-+\frac{b^4\gamma_u}{2}P_0,\\
\dot{P}_-&=-\left(1-\frac{b^2}{2}\right)\Gamma P_-+\frac{b^2\Gamma}{2}P_++\frac{b^4\gamma_u}{2}P_0.
\end{aligned} \tag{40}$$

Equations (40) have steady-state solutions,

$$P_0=\frac{a^2\Gamma}{a^2\Gamma+b^4\gamma_u},$$

$$P_+=P_-=\frac{1}{2}\frac{b^4\gamma_u}{a^2\Gamma+b^4\gamma_u}. \tag{41}$$

It is evident from Eq. (41) that for general γ_u and D all the dressed states are populated. In the absence of the dc field ($D=0$), the population $P_0=0$, and then the dynamics of the system reduces to that of a two-level system driven by a strong laser field. On the other hand, when either $\gamma_u=0$ or $D\gg\Omega$, the population is entirely trapped in the state $|0,N\rangle$.

With reference to Fig. 8, we see that, in the limit of well-separated lines, the total weight of the transition at frequency $\omega_L-\Omega'$ is given by $W(\omega-\omega_L)=P_0\gamma_{0+}+P_-\gamma_{-0}=W(\omega+\omega_L)$, the last step following by symmetry. Similarly, we find that $W(\omega_L\pm 2\Omega')=P_-\gamma_{-+}$ and $W(\omega_L)=P_0\gamma_{00}+P_-\gamma_{--}+P_+\gamma_{++}$.

To analyze the linewidths of the spectral lines, we study the time evolution of the off-diagonal density matrix elements

$$\rho_{ij}=\sum_N \rho_{i,N;j,N-1}. \tag{42}$$

First, we consider the outer sidebands at $\omega=\omega_L\pm 2\Omega'$. Projecting the master equation (7) onto $|-,N-1\rangle$ on the right and $\langle+,N|$ on the left, we obtain

$$\dot{\rho}_{+-}=-\left[i(\omega_L+2\Omega')+\left(1+\frac{1}{2}b^2\right)\Gamma\right]\rho_{+-}, \tag{43}$$

and similarly

$$\dot{\rho}_{-+}=-\left[i(\omega_L-2\Omega')+\left(1+\frac{1}{2}b^2\right)\Gamma\right]\rho_{-+}. \tag{44}$$

These coherences correspond to the spectral lines at $\omega-\omega_L=\pm 2\Omega'$. The widths of the lines are

$$\lambda_{\pm 2\Omega'}=\left(1+\frac{1}{2}b^2\right)\Gamma. \tag{45}$$

One can see that in the limit of $\gamma_u\ll\gamma_e$ the widths of the outer sidebands are independent of γ_u, which is in agreement with the numerical calculations of Sec. IV A.

For the inner sideband at $\omega_L+\Omega'$, we project the master equation onto $|0,N-1\rangle$ on the right and $\langle+,N|$ on the left. This results in two coupled equations,

$$\begin{aligned}
\dot{\rho}_{+0}&=-\left\{i(\omega_L+\Omega')+\frac{1}{2}[\Gamma+b^2(1+a^2)\gamma_u]\right\}\rho_{+0}\\
&\quad-\frac{1}{2}a^2b^2\gamma_u\rho_{0-},\\
\dot{\rho}_{0-}&=-\left\{i(\omega_L+\Omega')+\frac{1}{2}[\Gamma+b^2(1+a^2)\gamma_u]\right\}\rho_{0-}\\
&\quad-\frac{1}{2}a^2b^2\gamma_u\rho_{+0}.
\end{aligned} \tag{46}$$

The coherences corresponding to the left sideband at $\omega_L-\Omega'$ can be treated analogously, and it is easily to show that the coherences satisfy the same equations as Eq. (46), but with $\omega_L+\Omega'$ replaced by $\omega_L-\Omega'$.

In order to discuss the linewidths of the spectral components it is sufficient to find the real parts of the eigenvalues of the coupled equations (46), which are

$$\lambda_{\pm\Omega',1}=\frac{1}{2}(\Gamma+b^2\gamma_u),$$

$$\lambda_{\pm\Omega',2}=\frac{1}{2}[\Gamma+b^2(1+2a^2)\gamma_u]. \tag{47}$$

It is seen that the inner sidebands are composed of two lines of slightly different widths. (When nonzero detunings are allowed, it can be shown that the central frequencies of these two peaks may differ, resulting in the inner sidebands splitting into two peaks.)

Finally, we consider the central component of the spectrum. It is easily verified that there are three coherences oscillating at the same frequency ω_L which satisfy the following set of coupled equations:

$$\dot{\rho}_{00} = -(i\omega_L + b^4\gamma_u)\rho_{00} + a^2\Gamma(\rho_{++} + \rho_{--}),$$

$$\dot{\rho}_{++} = -\left[i\omega_L + \left(1 - \frac{1}{2}b^2\right)\Gamma\right]\rho_{++} + \frac{1}{2}b^2\Gamma\rho_{--} + \frac{1}{2}b^4\gamma_u\rho_{00},$$

$$\dot{\rho}_{--} = -\left[i\omega_L + \left(1 - \frac{1}{2}b^2\right)\Gamma\right]\rho_{--} + \frac{1}{2}b^2\Gamma\rho_{++} + \frac{1}{2}b^4\gamma_u\rho_{00}. \quad (48)$$

The eigenvalues of Eq. (48) are

$$\lambda_{c,1} = -i\omega_L,$$

$$\lambda_{c,2} = -i\omega_L - (a^2\Gamma + b^4\gamma_u),$$

$$\lambda_{c,3} = -i\omega_L - \Gamma. \quad (49)$$

The lowest eigenvalue corresponds to the elastic component of the spectrum, while the other eigenvalues correspond to the inelastic central component. Clearly, the central component is composed of two lines of different widths. For $D \ll 1$, the real part of $\lambda_{c,2}$ reduces to γ_u indicating that in the limit of $\gamma_u \ll \gamma_e$ the spectrum will exhibit a very narrow line at the central frequency, which is in agreement with the numerical calculations presented in Fig. 5. In the limit of $D \gg 1$ and $\gamma_u \ll \gamma_e$, the real parts of $\lambda_{c,2}$ and $\lambda_{c,3}$ both reduce to $\gamma_e/2$ indicating that in the limit of a strong coupling between the upper states, there are no sharp lines in the spectrum. This is in agreement with the numerical results presented in Fig. 7.

V. SUMMARY

We have proposed a practical scheme which permits the observation of the interesting features predicted for three-level systems showing strong quantum interference, but without the need for parallel dipole moments. In our system the transitions with perpendicular dipole moments are coupled by applying a dc field driving the transition between the upper atomic states. We have shown that the system can exhibit the features previously predicted for a system with parallel dipole moments: in particular, extraordinarily large values of the normalized intensity-intensity correlation function and ultranarrow lines in the resonance fluorescence spectrum. We have explained the spectral features in terms of the dressed-atom model of the system. Moreover, we have shown that the system can exhibit strong squeezing.

We conclude with some examples of possible experimental observations of the features predicted in this paper. A system with a metastable intermediate state, which is desirable for enhancing some of the features reported here (particularly ultrasharp lines) is atomic hydrogen, with the ground state being the $1s$ level, $|g\rangle \equiv |1s\rangle$, and the excited states being $|u\rangle \equiv |2s\rangle$,$|e\rangle \equiv |2p\rangle$, the 2s level being metastable [30]. The $2p$ spontaneous decay rate is $\gamma_e = 6.3 \times 10^8$ s^{-1}. We find $D \simeq 0.66 E_{dc}$ where E_{dc} is the externally applied dc field measured in kV cm^{-1}, so that a field of 7.7 kV cm^{-1} results in a value $D = 5\gamma_e$, as assumed in some of our figures.

The scheme used by Echaniz *et al.* [35] to observe a doubly driven V-type system might be suitable for demonstrating the quantum interference effects on transitions with perpendicular dipole moments. The scheme involves ^{87}Rb atoms cooled in a magneto-optics traps, with the states $|e\rangle$,$|u\rangle$, and $|g\rangle$ being the states $5P_{3/2}(F=0)$,$5P_{1/2}(F=2)$, and $5S_{1/2}(F=1)$, respectively. A polarized laser field drives the $5P_{3/2}(F=0) - 5S_{1/2}(F=1)$ transition with a dc field driving the $5P_{3/2}(F=0) - 5P_{1/2}(F=2)$ transition. The specific values of the dc field intensity are not crucial as the predicted effects are present for a weak as well as a strong dc field. The Rabi frequencies we have assumed here are quite modest, and we anticipate no difficulty in them being realized.

Another possibility is to use a V-type three-level system in solids, e.g., in Pr^{3+}:$YAlO_3$ [36]. In this system, the hyperfine transition $|\pm 1/2\rangle - |\pm 3/2\rangle$ in $^1D_2(0)$ may be chosen as the transition to be driven by a dc field. The dipole allowed transitions could be two of the $^3H_4(0) - {}^1D_2(0)$ transitions.

ACKNOWLEDGMENT

This research was supported in part by the University of Queensland Travel Awards for International Collaborative Research.

[1] G. S. Agarwal, in *Quantum Statistical Theories of Spontaneous Emission and their Relation to Other Approaches*, edited by G. Höhler, Springer Tracts in Modern Physics Vol. 70 (Springer, Berlin, 1974).

[2] D. A. Cardimona, M. G. Raymer, and C. R. Stroud, Jr., J. Phys. B **15**, 65 (1982).

[3] G. C. Hegerfeldt and M. B. Plenio, Phys. Rev. A **46**, 373 (1992).

[4] P. Zhou and S. Swain, Phys. Rev. Lett. **77**, 3995 (1996); Phys. Rev. A **56**, 3011 (1997).

[5] S.-Y. Zhu and M. O. Scully, Phys. Rev. Lett. **76**, 388 (1996).

[6] H. Lee, P. Polynkin, M. O. Scully, and S. Y. Zhu, Phys. Rev. A **55**, 4454 (1997); F.-L. Li and S.-Y. Zhu, *ibid.* **59**, 2330 (1999).

[7] K. J. Boller, A. Imamoglu, and S. E. Harris, Phys. Rev. Lett. **66**, 2593 (1991); K. Hakuta, L. Marmet, and B. Stoicheff, *ibid.* **66**, 596 (1991); J. C. Petch, C. H. Keitel, P. L. Knight, and J. P. Marangos, Phys. Rev. A **53**, 543 (1996).

[8] S. E. Harris, Phys. Rev. Lett. **62**, 1033 (1989); M. O. Scully, S.-Y. Zhu, and A. Gavrielides, *ibid.* **62**, 2813 (1989); G. S. Agarwal, Phys. Rev. A **44**, R28 (1991); C. H. Keitel, O. Ko-

charovskaya, L. M. Narducci, M. O. Scully, S.-Y. Zhu, and H. M. Doss, *ibid.* **48**, 3196 (1993); P. Zhou and S. Swain, Phys. Rev. Lett. **78**, 832 (1997); J. Kitching and L. Hollberg, Phys. Rev. A **59**, 4685 (1999).

[9] A. K. Patnaik and G. S. Agarwal, J. Mod. Opt. **45**, 2131 (1998); E. Paspalakis, C. H. Keitel, and P. L. Knight, Phys. Rev. A **58**, 4868 (1998); S. Menon and G. S. Agarwal, *ibid.* **57**, 4014 (1998); S.-Q. Gong, E. Paspalakis, and P. L. Knight, J. Mod. Opt. **45**, 2433 (1998).

[10] C. H. Keitel, Phys. Rev. Lett. **83**, 1307 (1999).

[11] S. Swain, P. Zhou, and Z. Ficek, Phys. Rev. A **61**, 043410 (2000).

[12] U. Akram, Z. Ficek, and S. Swain, Phys. Rev. A **62**, 013413 (2000).

[13] G. C. Hegerfeldt and M. B. Plenio, Phys. Rev. A **47**, 2186 (1993).

[14] A. S. Manka, E. J. D'Angelo, L. M. Narducci, and M. O. Scully, Phys. Rev. A **47**, 4236 (1993).

[15] L. M. Narducci, M. O. Scully, G.-L. Oppo, P. Ru, and J. R. Tredicci, Phys. Rev. A **42**, 1630 (1990).

[16] R. J. Cook and H. J. Kimble, Phys. Rev. Lett. **54**, 1023 (1985).

[17] D. T. Pegg, R. Loudon, and P. L. Knight, Phys. Rev. A **33**, 4085 (1986).

[18] M. Wiegand, J. Phys. B **16**, 1133 (1983).

[19] M. Jakob, Y. Abranyos, and J. A. Bergou, J. Opt. B: Quantum Semiclassical Opt. **3**, 130 (2001).

[20] H. R. Xia, C. Y. Ye, and S. Y. Zhu, Phys. Rev. Lett. **77**, 1032 (1996).

[21] Li Li, X. Wang, J. Yang, G. Lazarov, J. Qi, and M. M. Lyyra, Phys. Rev. Lett. **84**, 4016 (2000).

[22] P. R. Berman, Phys. Rev. A **58**, 4886 (1998).

[23] J. Wang, H. M. Wiseman, and Z. Ficek, Phys. Rev. A **62**, 013818 (2000).

[24] B. M. Garraway and P. L. Knight, Phys. Rev. A **54**, 3592 (1996).

[25] A. K. Patnaik and G. S. Agarwal, Phys. Rev. A **59**, 3015 (1999).

[26] P. Zhou and S. Swain, Opt. Commun. **179**, 267 (2000).

[27] P. Zhou, S. Swain, and L. You, Phys. Rev. A **63**, 033818 (2001).

[28] G. S. Agarwal, Phys. Rev. Lett. **84**, 5500 (2000).

[29] B. J. Dalton and M. Gagen, J. Phys. B **18**, 4403 (1985).

[30] K. Hakuta, L. Marmet, and B. P. Stoicheff, Phys. Rev. A **45**, 5152 (1992).

[31] D. J. Gauthier, Yifu Zhu, and T. W. Mossberg, Phys. Rev. Lett. **66**, 2460 (1991).

[32] B. N. Jagatap, Q. V. Lawande, and S. V. Lawande, Phys. Rev. A **43**, 535 (1991).

[33] H. Huang, S.-Y. Zhu, M. S. Zubairy, and M. O. Scully, Phys. Rev. A **53**, 1834 (1996).

[34] C. Cohen-Tannoudji and S. Reynaud, J. Phys. B **10**, 345 (1977); C. Cohen-Tannoudji, J. Dupont-Roc, and G. Grynberg, *Atom-Photon Interactions* (Wiley, New York, 1992).

[35] S. R. de Echaniz, A. D. Greentree, A. V. Durrant, D. M. Segal, J. P. Marangos, and J. A. Vaccaro, Phys. Rev. A **64**, 013812 (2001).

[36] K. Yamamoto, K. Ichimura, and N. Gemma, Phys. Rev. A **58**, 2460 (1998).